

# RSC Advances



This is an *Accepted Manuscript*, which has been through the Royal Society of Chemistry peer review process and has been accepted for publication.

*Accepted Manuscripts* are published online shortly after acceptance, before technical editing, formatting and proof reading. Using this free service, authors can make their results available to the community, in citable form, before we publish the edited article. This *Accepted Manuscript* will be replaced by the edited, formatted and paginated article as soon as this is available.

You can find more information about *Accepted Manuscripts* in the [Information for Authors](#).

Please note that technical editing may introduce minor changes to the text and/or graphics, which may alter content. The journal's standard [Terms & Conditions](#) and the [Ethical guidelines](#) still apply. In no event shall the Royal Society of Chemistry be held responsible for any errors or omissions in this *Accepted Manuscript* or any consequences arising from the use of any information it contains.

# Real-space characterization of hydroxyphenyl porphyrin derivatives designed for single-molecule devices

Akitoshi Shiotari,<sup>1,\*</sup> Yusuke Ozaki,<sup>1</sup> Shoichi Naruse,<sup>1</sup> Hiroshi Okuyama,<sup>1,†</sup> Shinichiro Hatta,<sup>1</sup> Tetsuya Aruga,<sup>1</sup> Takashi Tamaki,<sup>2</sup> and Takuji Ogawa<sup>2</sup>

<sup>1</sup>*Department of Chemistry, Graduate School of Science, Kyoto University, Kyoto 606-8502, Japan. Fax: +81 75 753 4000; Tel: +81 75 753 3977*

<sup>2</sup>*Department of Chemistry, Graduate School of Science, Osaka University, 1-1 Machikaneyama-cho, Toyonaka, Osaka 560-0043, Japan.*

(Dated: August 20, 2015)

## Abstract

The porphyrin derivatives are potential candidates as constituents of functional molecular devices because their electronic levels can rationally be manipulated by chemical modification. In this work, we deposit a porphyrin molecule with a hydroxyphenyl side group on Au(111), which is designed and synthesized as a basic unit for functional single molecule devices, and observe the bonding structure and electronic states with a scanning tunneling microscope (STM). The molecule changes the configuration from monomer, cluster to monolayer as the coverage increases, ruled by the H-bonding interaction through the hydroxyphenyl group and steric repulsion by isopentoxy groups. The highest occupied molecular orbital (HOMO) and the lowest unoccupied molecular orbital (LUMO) localized in the porphyrin macrocycle are observed at  $-1.1$  and  $+1.1$  eV, respectively, with respect to the Fermi level. We also deposit a *para*-phenylene-bridged porphyrin array on the surface by electro spray method, and observe the local density of states along the array.

---

\* Present address: Department of Advanced Materials Science, The University of Tokyo, Kashiwa 277-8561, Japan

† Corresponding author: hokuyama@kuchem.kyoto-u.ac.jp

## I. INTRODUCTION

Porphyrins and the related macrocycles have rich optical and redox properties, which can be modulated by appropriate metalation. The flexible tunability of their properties makes them potential for molecular electronics applications.<sup>1-5</sup> Recently, Tamaki et al.<sup>6</sup> reported a methodology for the synthesis of porphyrin arrays with programmed sequence. Because the individual porphyrin macrocycle possesses localized valence state of distinct energy levels, it is possible to engineer the distribution of the frontier orbitals along the array, and thereby to rationally design the transport property through the molecule. The electronic states of the arrayed molecules were studied by using optical and electrochemical methods, which revealed the highest occupied molecular orbital (HOMO) and the lowest unoccupied molecular orbital (LUMO) levels of each component. However, these versatile techniques are not able to probe the electronic states in a site-resolved way; it is essential to investigate the spatial distribution of the frontier orbitals along the array for the control of the transport property through the molecules.

A scanning tunneling microscope (STM) is useful to investigate the electronic states and its spatial distribution for the molecules on the surface. The adsorption and self-assembly of porphyrin derivatives on surfaces have been intensively studied, mainly for the understanding of molecule-electrode interaction, which is essential for their application to molecular electronics.<sup>7-13</sup> Not only the giant molecules,<sup>14-16</sup> but also the functional molecules, such as molecular switches<sup>17,18</sup> and molecular magnet,<sup>19</sup> were imaged and characterized at a single-molecule level. In this work, using STM, we image hydroxyphenyl porphyrin unit and its array which are synthesized as the basis of molecular rectifier, and characterize the electronic state associated with the transport property through the molecule.

## II. EXPERIMENTAL

The STM experiments were carried out in an ultrahigh-vacuum chamber (USM-1200, Unisoku). An electrochemically etched tungsten tip was used as an STM probe. The STM images were acquired in constant current mode at 6 K. Single-crystalline Au(111) was cleaned by repeated cycles of Ar<sup>+</sup> sputtering and annealing.

10-(4-Hydroxyphenyl)-5,15-bis(3,5-diisopentoxyphenyl) freebase porphyrin (FbP; Fig. 1a)

and *para*-phenylene-bridged porphyrin array of Zn porphyrin [(ZnP)<sub>3</sub>; Fig. 1b] were synthesized according to the previous work.<sup>6</sup> The FbP molecules were thermally sublimated from a stainless crucible at  $\sim 540$  K and deposited to the surface kept at  $\sim 90$  K. We also used an electrospray ionization method (ADCAP vacuum technology, Japan) to deposit nonvolatile (ZnP)<sub>3</sub> onto the surface.<sup>20</sup> The molecule was dissolved in 10:1 methanol/toluene (by volume) mixture to give a concentration of  $49 \mu\text{M}$ . The solution in the atmosphere was introduced into a differential pumping chamber at a typical flow rate of  $2 \mu\text{L}/\text{min}$  through a needle tube with an applied voltage of 1.4 kV. The Au(111) surface was exposed to the ion flux (typical ion current of 10–30 pA) for 5 min at room temperature.

The  $dI/dV$  curves were obtained by using a lock-in amplifier with a modulation voltage of  $8 \text{ mV}_{\text{rms}}$  at 590 Hz. Each spectrum is displayed after subtraction of  $dI/dV$  obtained over the clean surface obtained at the constant tip height.

### III. RESULTS AND DISCUSSION

#### A. Porphyrin monomer

Fig. 2 shows STM images of FbP molecules on Au(111) as a function of coverage. The molecules were adsorbed on the surface at  $\sim 90$  K. At low coverage (Fig. 2a), the molecules are bonded to the elbow sites of the herringbone structure,<sup>21</sup> in a similar way to other porphyrin derivatives on the surface.<sup>22,23</sup> The molecule surrounded by the dotted ellipse is assigned to an isolated molecule (described below), and their clusters are also observed at the elbow sites. In case the surface was exposed to the molecules at room temperature, they were trapped at the step edges on the surface (not shown). The molecules diffused across the surface and migrated to more favorable step sites at room temperature. Therefore it is essential to maintain the surface at  $\sim 90$  K to isolate the molecules on the terrace of the surface. As the coverage increases, the molecules form islands in the face-centered-cubic region of the herringbone structure (Fig. 2b), and eventually forms a monolayer over the surface (Fig. 2c).

Fig. 3a shows close inspection into an isolated molecule. The image consists of a ring surrounded by four spots (green dots) and one spot indicated by an arrow. By comparison with the molecular structure (Fig. 3b), we assign the center ring to a porphyrin macrocycle,

and the four spots to the isopentoxy groups (green ellipses in Fig. 3b). The arrow indicates the hydroxyphenyl group (yellow ellipse in Fig. 3b). During successive scans, the appearance and position of the four isopentoxy moieties (green dots) change independently, as shown in Fig. 3a, c, and d. The fluctuation is ascribed to the rotation of the isopentoxy moieties around the  $sp^3$  C–C bonds, which is induced by the interaction with the STM tip; it depends on the tunnel condition. We could not suppress the motion under the condition employed ( $V = 0.03$ – $2$  V and  $I = 10$ – $500$  pA).

Fig. 3e and f show STM images of the molecule obtained at  $V = +1.5$  and  $-1.5$  V, respectively. Depending on the bias voltage, the appearance of the macrocycle drastically changes. It appears as a rather uniform ring at low bias (Fig. 3a), but the upper part of the ring becomes more protruded at  $V = +1.5$  V (Fig. 3e). Note that the upper part of the image corresponds to the site to which the hydroxyphenyl group is bonded (yellow ellipse in Fig. 3b). When the bias polarity is reversed ( $V = -1.5$  V), the bright feature is localized at the specific position of the ring (the cross in Fig. 3f). The dependence of the image on the bias voltage is ascribed to energy distribution of the electronic states of the molecule. Fig. 3g shows a normalized  $dI/dV$  spectrum [i.e.,  $(\frac{dI}{dV}) / (\frac{I}{V})$  curve] obtained over the cross in Fig. 3f. The density-functional theory (DFT) calculation for the free FbP molecule showed that LUMO and the second lowest unoccupied molecular orbital (LUMO+1) are distributed within  $0.04$  eV<sup>6</sup> and thus may contribute to a peak at  $V = +1.1$  V. HOMO and the second highest occupied molecular orbital (HOMO–1) are separated from each other by  $0.4$  eV for the free molecule<sup>6</sup> and thus contribute to peaks at  $V = -1.1$  and  $-1.6$  V, respectively. Therefore, the STM images obtained at  $V = +1.5$  V (Fig. 3e) and  $V = -1.5$  V (Fig. 3f) reflect the shape of LUMO–LUMO+1 and HOMO–HOMO–1 of the molecule, respectively. The HOMO–LUMO gap of  $\sim 2.2$  eV is narrower than the calculated value for the free molecule ( $2.7$  eV).<sup>6</sup> The reduction of the gap is possibly ascribed to surface polarization effects.<sup>24–26</sup>

Fig. 4a shows the STM image of dimerized FbP molecules. The molecules preferentially form clusters and islands, as shown in Fig. 2b, suggesting the presence of attractive interaction between the molecules. In Fig. 4a, the molecules in the dimer are interacted with each other via hydroxyphenyl groups (head-to-head configuration), as illustrated in Fig. 4b. In analogy to similar alkoxyphenyl-substituted cyanophenyl porphyrin,<sup>22,27</sup> we attribute the interaction to H-bonding between the hydroxyl group and  $\beta$ -hydrogen of the

adjacent porphyrin ring. Note that STS measured over the dimerized FbP (not shown) has the same structure as that of an isolated FbP molecule (Fig. 3g), suggesting that the frontier orbitals are not affected by the H-bonds. At higher coverage the molecules form a monolayer, as shown in Fig. 4c. On the terrace of the surface, the molecules are arranged in a quasi-rectangular arrangement with the hydroxyphenyl groups pointing random in opposite direction (Fig. 4d). This is consistent with the  $\beta$ -H $\cdots$ OH interaction; the head-to-tail configuration (one H-bond) is nearly degenerate with simultaneous head-to-head (two H-bonds) and tail-to-tail (no H-bond) configurations. Therefore, we suggest that the structure of the monolayer is mainly determined by the interaction between the side isopentoxy groups; the molecules are densely packed by avoiding steric repulsion between them.

## B. Porphyrin array

A variety of metallated porphyrin units can be linked via phenylene in programmed sequence, enabling one to tailor the transport property through the molecule.<sup>6</sup> Here, as a first step toward the characterization of programmed arrays, we deposit a homologous porphyrin array [(ZnP)<sub>3</sub>] on the surface and observe the electronic state at a level of individual molecules. Fig. 5a shows typical STM images of (ZnP)<sub>3</sub> deposited by electro spray method on Au(111). Isolated molecules and clusters are observed. Fig. 5b shows a magnified image of an isolated (ZnP)<sub>3</sub> molecule. The image is consistent with the molecular structure (Fig. 1b), as illustrated in Fig. 5c. The individual macrocycles with four isopentoxy groups are shown by the red, green, and blue envelopes, corresponding to the head, center, and tail macrocycles, respectively. The residual protrusions (outside of the envelopes) were not reproducible, and thus, are ascribed to impurities attached to the molecule coadsorbed during the electro spray deposition (possibly solvent molecules).

The electronic states of (ZnP)<sub>3</sub> are investigated with STM as shown in Fig. 5d. The red, green, and blue curves show normalized  $dI/dV$  curves obtained over the position marked by the crosses of corresponding colors in Fig. 5e. The  $dI/dV$  shows the local density of states of the frontier orbitals at each site. As for the unoccupied states, a peak is observed at 1.3 V. The DFT calculation for the free (ZnP)<sub>3</sub> molecule showed that five orbitals (LUMO–LUMO+5) are distributed within 0.1 eV<sup>6</sup> and thus may contribute to the peak. As for the occupied states, the  $dI/dV$  of the head and tail macrocycles shows a broad feature around –1

V, while that of the center macrocycle shows characteristic split structure. The calculation showed that HOMO–HOMO–5 are distributed within 0.3 eV<sup>6</sup> and thus contribute to these structures. The site-dependent  $dI/dV$  is ascribed to the distribution of so many orbitals along the array. Note that these orbitals may be perturbed by the substrate as well as by the deformation (described later). Therefore DFT calculations for adsorbed  $(\text{ZnP})_3$  would help the interpretation of the site-dependent  $dI/dV$ .

The image obtained at  $V = +1.5$  V (Fig. 5e) is contributed from LUMO–LUMO+5, where the macrocycles show complex internal structure as depicted in Fig. 5f. The image obtained at  $V = -1.5$  V reflects the shape of overall HOMO–HOMO–5 (Fig. 5g). The illustration of the occupied-state image (Fig. 5h) shows that each porphyrin macrocycle is no longer symmetric with respect to the molecular axis. The Zn atoms are positioned at the center of the cavities, and thus, we suggest that the asymmetry is due to the deformation of the macrocycles. Indeed, it was suggested that the macrocycle is deformed into saddle shape with pairs of opposite pyrrole tilted upward or downward to increase the interaction with the surfaces,<sup>17,22–24,27–30</sup> which is consistent with the image in Fig. 5h. The two salient protrusions in the molecular image (Fig. 5b) is possibly ascribed to the isopentoxo groups tilted upward according to the deformation of the macrocycles.

#### IV. CONCLUSION

We image a freebase porphyrin monomer (FbP) and zinc porphyrin array  $[(\text{ZnP})_3]$  on Au(111), and characterize their electronic states with STM. The nonvolatile porphyrin array is successfully deposited on the surface using an electrospray deposition. The STM reveals the energy level and spatial distribution of the frontier orbitals localized on the individual porphyrin macrocycles in the molecules. The real-space imaging is also useful for studying their aggregation on the surface. Combined with nondestructive deposition method, the STM can probe the local electronic states along the programmed porphyrin arrays, which is associated with the transport property through the molecule.

## ACKNOWLEDGMENTS

This study was supported in part by Grant-in-Aid for Scientific Research on Innovative Areas “Molecular Architectonics: Orchestration of Single Molecules for Novel Functions.” A.S. acknowledges the support of the Japan Society for the Promotion of Science. The authors acknowledge T. Yokoyama for technical support of the electrospray deposition.



- 
- [1] M. Jurow, A. E. Schuckman, J. D. Batteas and C. M. Drain, *Coord. Chem. Rev.*, 2010, **254**, 2297–2310.
- [2] H. Xu, R. Chen, Q. Sun, W. Lai, Q. Su, W. Huang and X. Liu, *Chem. Soc. Rev.*, 2014, **43**, 3259–3302.
- [3] K. Tagami, M. Tsukuda, T. Matsumoto and T. Kawai, *Phys. Rev. B*, 2003, **67**, 245324.
- [4] J. A. A. W. Elemans, R. van Hameren, R. J. M. Norte and A. E. Rowan, *Adv. Mater.*, 2006, **18**, 1251–1266.
- [5] G. Sedghi, V. M. García-Suárez, L. J. Esdaile, H. L. Anderson, C. J. Lambert, S. Martin, D. Bethell, S. J. Higgins, M. Elliott, N. Bennett, J. E. Macdonald and R. J. Nichols, *Nat. Nanotech.*, 2011, **6**, 517–523.
- [6] T. Tamaki, T. Nosaka and T. Ogawa, *J. Org. Chem.*, 2014, **79**, 11029–11038.
- [7] J. Otuski, *Coord. Chem. Rev.*, 2010, **254**, 2311–2341.
- [8] S. Mohnani and D. Bonifazi, *Coord. Chem. Rev.*, 2010, **254**, 2342–2362.
- [9] S. Yoshimoto and N. Kobayashi, *Struct. Bond.*, 2010, **135**, 137–168.
- [10] J. Xiao, S. Ditze, M. Chen, F. Buchner, M. Stark, M. Drost, H.-P. Steinrück, J.M. Gottfried and H. Marbach, *J. Phys. Chem. C*, 2012, **116**, 12275–12282.
- [11] T. Niu and A. Li, *J. Phys. Chem. Lett.*, 2013, **4**, 4095–4102.
- [12] S. Haq, F. Hanke, J. Sharp, M. Persson, D.B. Amabilino and R. Raval, *ACS Nano*, 2014, **9**, 8856–8870.
- [13] W. Auwärter, D. Écija, F. Klappenberger and J. V. Barth, *Nat. Chem.*, 2015, **7**, 105–120.
- [14] A. Saywell, J. K. Sprafke, L. J. Esdaile, A. J. Britton, A. Rienzo, H. L. Anderson, J. N. O’Shea and P. H. Beton, *Angew. Chem. Int. Ed.*, 2010, **49**, 9136–9139.
- [15] M. C. O’Sullivan, J. K. Sprafke, D. V. Kondratuk, C. Rinfray, T. D. W. Claridge, A. Saywell, M. O. Blunt, J. N. O’Shea, P. H. Beton, M. Malfois and H. L. Anderson, *Nature*, 2011, **469**, 72–75.
- [16] D. V. Kondratuk, L. M. A. Perdigao, M. C. O’Sullivan, S. Svatek, G. Smith, J. N. O’Shea, P. H. Beton and H. L. Anderson, *Angew. Chem. Int. Ed.*, 2012, **51**, 6696–6699.
- [17] W. Auwärter, K. Seufert, F. Bischoff, D. Ecija, S. Vijayaraghavan, S. Joshi, F. Klappenberger, N. Samudrala and J. V. Barth, *Nat. Nanotech.*, 2012, **7**, 41–46.

- [18] S. Ditze, M. Stark, F. Buchner, A. Aichert, N. Jux, N. Luckas, A. Görling, W. Hieringer, J. Hornegger, H.-P. Steinrück and H. Marbach, *J. Am. Chem. Soc.*, 2014, **136**, 1609–1616.
- [19] W. Wang, R. Pang, G. Kuang, X. Shi, X. Shang, P.N. Liu and N. Lin, *Phys. Rev. B*, 2015, **91** 045440.
- [20] T. Yokoyama, Y. Kogure, M. Kawasaki, S. Tanaka and K. Aoshima, *J. Phys. Chem. C*, 2013, **117**, 18484–18487.
- [21] J. V. Barth, H. Brune, G. Ertl and R. J. Behm, *Phys. Rev. B*, 1990, **42**, 9307–9318.
- [22] T. Yokoyama, S. Yokoyama, T. Kamikado, Y. Okuno and S. Mashiko, *Nature*, 2001, **413**, 619–621.
- [23] T. Yokoyama, S. Yokoyama, T. Kamikado and S. Mashiko, *J. Chem. Phys.*, 2001, **115**, 3814–3818.
- [24] A. Weber-Bargioni, W. Auwärter, F. Klappenberger, J. Reichert, S. Lefrançois, T. Strunskus, C. Wöll, A. Schiffrin, Y. Penneç and J. V. Barth, *Chem. Phys. Chem.*, 2008, **9**, 89–94.
- [25] J. B. Neaton, M. S. Hybertsen and S. G. Louie, *Phys. Rev. Lett.*, 2006, **97**, 216405.
- [26] G. Heimel and J.-L. Bredas, *Nat. Nanotech.*, 2013, **8**, 230–231.
- [27] N. Wintjes, J. Hornung, J. Lobo-Checa, T. Voigt, T. Samuely, C. Thilgen, M. Stöhr, F. Diederich and T. A. Jung, *Chem. Eur. J.*, 2008, **14**, 5794–5802.
- [28] F. Buchner, K. Comanici, N. Jux, H.-P. Steinrück and H. Marbach, *J. Phys. Chem. C*, 2007, **111**, 13531–13538.
- [29] W. Auwärter, K. Seufert, F. Klappenberger, J. Reichert, A. Weber-Bargioni, A. Verdini, D. Cvetko, M. Dell’Angela, L. Floreano, A. Cossaro, G. Bavdek, A. Morgante, A. P. Seitsonen and J. V. Barth, *Phys. Rev. B*, 2010, **81**, 245403.
- [30] T. Yokoyama and F. Nishiyama, *J. Phys. Chem. Lett.*, 2014, **5**, 1324–1328.

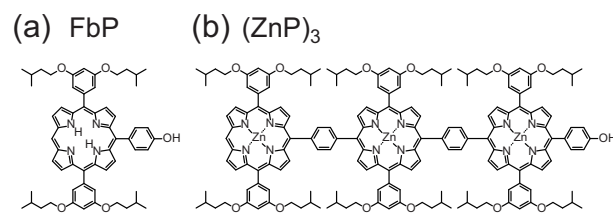


FIG. 1. Molecular structures of (a) a freebase porphyrin monomer (FbP) and (b) phenylene-linked Zn porphyrin array [(ZnP)<sub>3</sub>].

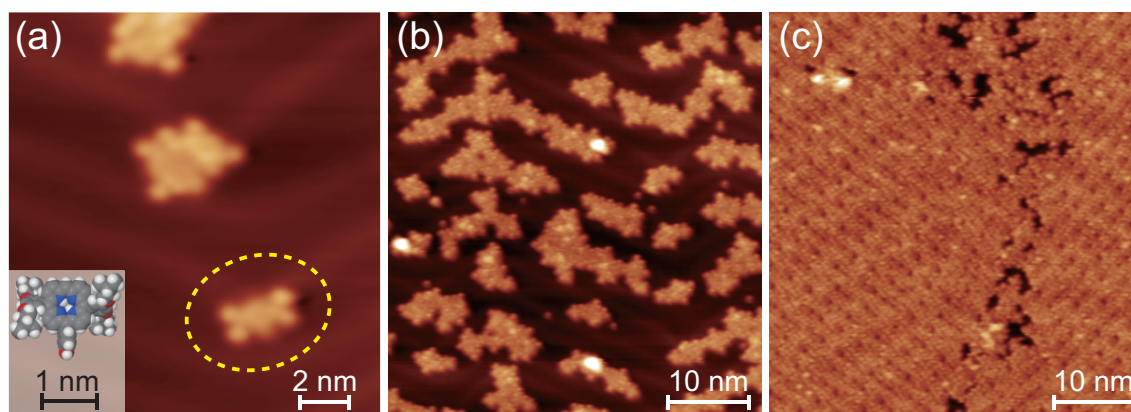


FIG. 2. (a)–(c) Typical STM images of freebase porphyrin monomers (FbP) on Au(111) as a function of coverage ( $V = +0.4$  V and  $I = 50$  pA). The dotted ellipse in (a) indicates an isolated molecule. The inset in (a) represents a calculated structure of a free FbP molecule (b3lyp/6-31G). The black, blue, red, and white spheres represent C, N, O, H atoms, respectively.

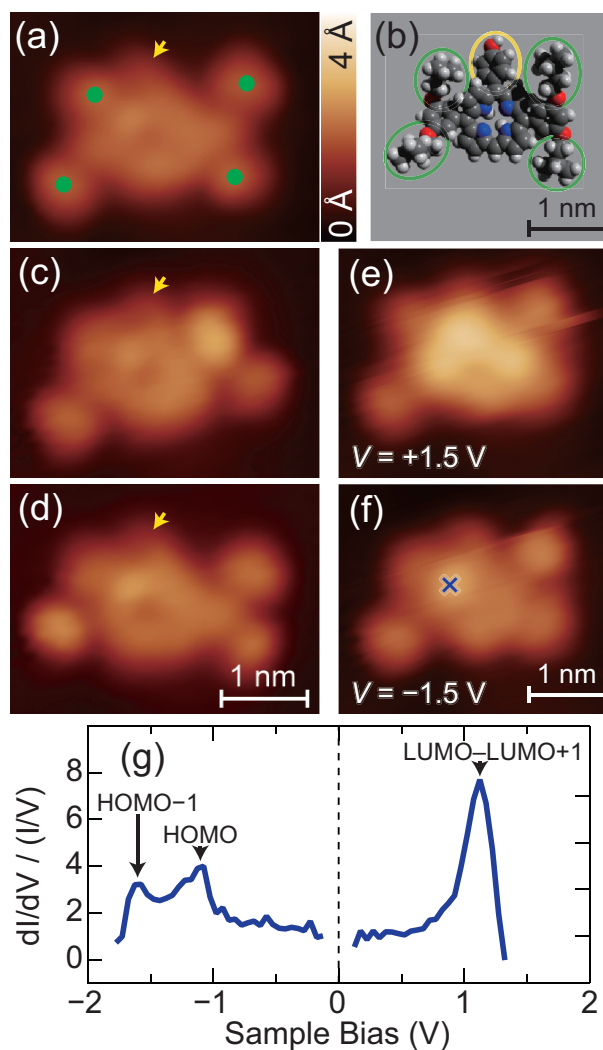


FIG. 3. (a) STM images of an isolated FbP molecule ( $V = +0.4$  V and  $I = 50$  pA). The green dots indicate the isopentoxy groups. (b) Schematic illustration of the molecular structure for a FbP molecule. The green and yellow ellipses indicate the isopentoxy and hydroxyphenyl groups, respectively. (c),(d) STM images of the same molecule as (a), sequentially recorded under the same condition. The arrows in (a), (c), and (d) indicate the hydroxyphenyl group. (e),(f) STM images of the same molecule as (a), acquired with  $V =$  (d)  $+1.5$  and (e)  $-1.5$  V at  $I = 50$  pA. (g) A normalized  $dI/dV$  spectrum of the FbP molecule recorded over the cross in (f). The black arrows represent resonance peaks of the molecular orbitals.

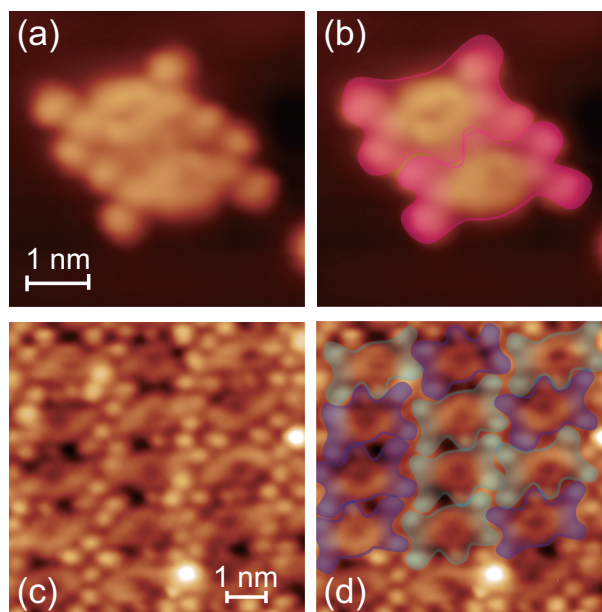


FIG. 4. (a),(c) The STM images of (a) dimerized FbP molecules and (c) monolayer FbP ( $V = +0.4$  V and  $I = 50$  pA). (b),(d) The same as (a) and (c), respectively, superimposed by the envelopes representing the contour of the molecules. Blue and cyan envelopes in (d) represent the molecules which are rotated by  $180^\circ$  with each other.

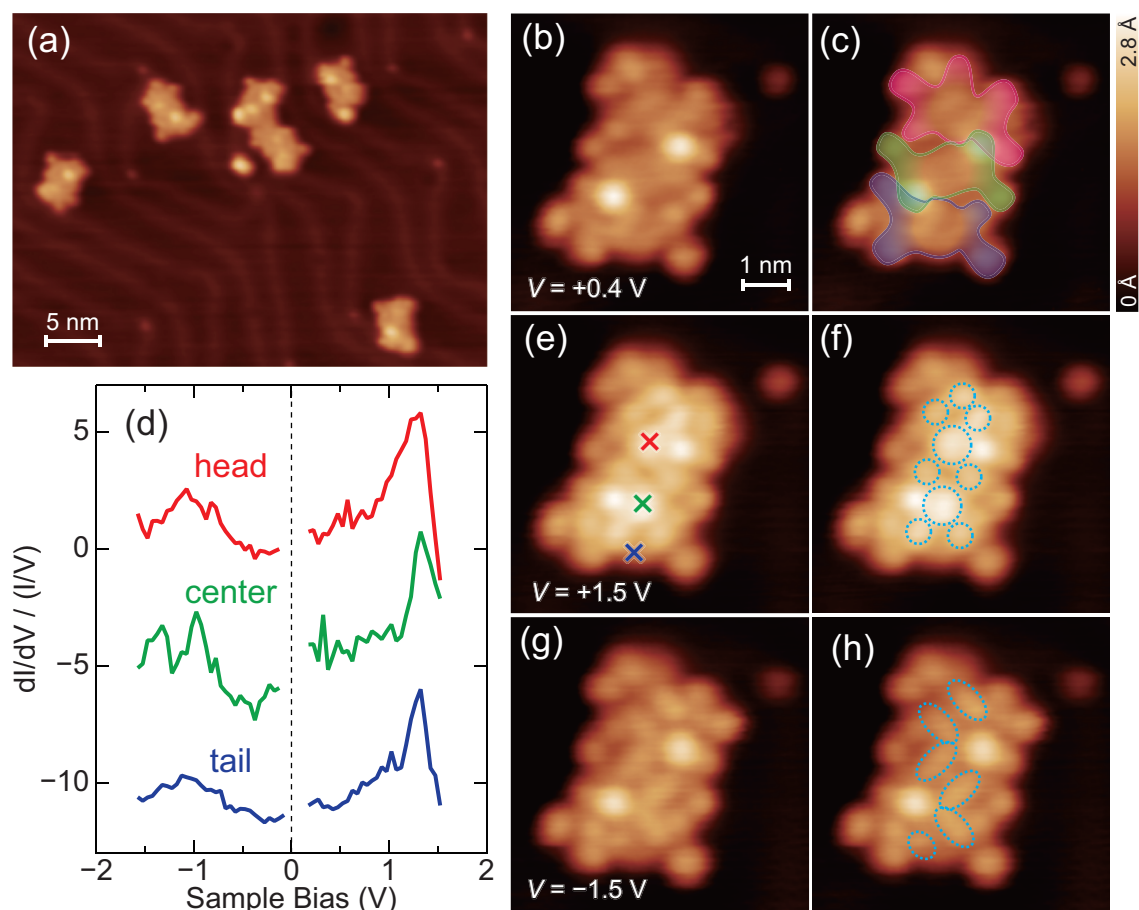


FIG. 5. (a) Typical STM images of zinc porphyrin arrays  $[(\text{ZnP})_3]$  on Au(111) ( $V = +0.4$  V and  $I = 50$  pA). (b),(e),(g) close-up images of an array acquired with  $V =$  (a)  $+0.4$ , (e)  $+1.5$ , and (g)  $-1.5$  V at  $I = 50$  pA. (c) The same as (b) superimposed by the envelopes representing the contour of each component. (d) Normalized  $dI/dV$  curves of the array (offset for clarity). The red, green, and blue curves are recorded over the position marked by the crosses of corresponding colors in (e). (f),(h) The same as (e) and (g), respectively, superimposed by the ellipses illustrating the shape of the orbitals distributed in each macrocycle.